Finite temperature magnetic properties of small Fe chains and clusters on Pt(111)

S. Riemer,[1] J. Dorantes-Dávila,[2] and G. M. Pastor[1]
[1]*Institut für Theoretische Physik, Universität Kassel, 34132 Kassel, Germany*
[2]*Instituto de Física, Universidad Autónoma de San Luis Potosí, 78000 San Luis Potosí, Mexico*
(Received 4 December 2015; revised manuscript received 25 February 2016; published 11 April 2016)

The magnetic properties of Fe chains and clusters on Pt(111) are investigated in the framework of a functional-integral theory of itinerant magnetism. The considered nanostructures show a ferromagnetic (FM) ground state with nearly saturated Fe local magnetic moments $\mu^0_{\rm Fe} \simeq 3.15\mu_{\rm B}$. In addition, small moments $\mu^0_{\rm Pt} \simeq 0.1$–$0.3\mu_{\rm B}$ are induced at the Pt substrate, which depend sensitively on the number of Fe atoms in their nearest-neighbor (NN) shell. The spin-fluctuation (SF) energies $\Delta F_l(\xi)$ at the different atoms l are calculated as a function of the local exchange fields ξ_l, by using a real-space recursive expansion of the local Green's functions. Results for the temperature dependence of the average magnetization per atom $\overline{\mu}_N$, local magnetic moments μ_l, and spin correlation functions γ_{lk} are derived. At the Fe atoms the dominant magnetic excitations are fluctuations of the local-moment orientations. The spin-flip energies $\Delta F_l(\xi)$ in the deposited Fe clusters are found to be about 50% smaller than in free-standing clusters of comparable size. This results in flatter SF-energy landscapes and in a weaker stability of the FM order at $T > 0$. The effective exchange interactions between the Fe local moments, which are derived from the electronic calculations, reveal competing FM and antiferromagnetic couplings at different distances. In contrast to Fe, the main spin excitations at the Pt atoms are fluctuations of the size of the induced local magnetic moments. The interplay between the different types of spin excitations and their effect on the temperature-dependent magnetic properties is discussed.

DOI: 10.1103/PhysRevB.93.134414

I. INTRODUCTION

The magnetic behavior of nanostructured transition metals (TMs) remains the subject of a remarkably intense research activity from both fundamental and technological perspectives [1–10]. One of the major driving forces in this field is the possibility of modifying and controlling the fundamental properties of magnetic materials—magnetic moments, magnetic order, magnetic anisotropy, etc.—by systematic manipulation of their size, composition, structure, and dimensionality. The well-documented strong sensitivity of the dominant 3*d* states on the local environment of the atoms [11–16] offers indeed a wide variety of opportunities to unravel interesting effects with important potential applications [1–6].

The temperature dependence of the magnetic properties is a particularly challenging and important issue in this context. Temperature plays a fundamental role in the behavior of correlated itinerant 3*d* electrons, most obviously concerning the fluctuations of the spin degrees of freedom and the magnetic order. But in addition, controlling temperature effects is crucial in view of almost any technological use of magnetic materials. Besides the more traditional situation of thermodynamic equilibrium, increasing attention has been recently paid to the magnetic response of TM compounds after localized intense excitation, for example, by means of ultrashort laser pulses [10]. Consequently, the prospects of manipulating the spin-polarized electronic density in a space- and time-resolved way raises considerably the importance of understanding the nature of the magnetic excitations in nanostructures.

Simple general trends on the finite temperature behavior as a function of composition and structure are difficult to infer *a priori*. In fact, the valence *d* electrons, which give the dominant contribution to TM magnetism, are particularly sensitive to the local environment of the atoms and to the variables that define it [e.g., local coordination numbers, nearest-neighbor (NN) distances, chemical composition of the NN shells, etc.]. Reliable conclusions concerning the size of the local magnetic moments, their couplings, and the stability of magnetic order at finite temperature should be therefore based on an electronic theory, which takes into account both itinerant character of the *d*-electron states and the important Coulomb interactions responsible for local moment formation. Simple phenomenological spin Hamiltonians, such as the Heisenberg, *xy*, or Ising models, are not expected to be very predictive, unless they incorporate the electronic effects behind the effective couplings between the local magnetic degrees of freedom [17–20].

Previous theoretical studies on free-standing and supported clusters and nanostructures have already revealed a number of interesting effects concerning the ground-state and finite-temperature magnetic properties as a function of size, structure, and interatomic distances [11,18,19,21–24]. For instance, Šipr *et al.* have investigated gas-phase Fe_N clusters having $N = 9$–89 atoms by combining a classical Heisenberg spin model with the exchange couplings derived from density-functional calculations [19]. In this way, the temperature scale $T_C(N)$, at which the average cluster magnetization decreases significantly, has been identified. Trends as a function of size have been inferred. In addition, electronic calculations on the finite temperature properties of Fe and Ni clusters and ultrathin films have been performed in the framework of a spin-fluctuation theory of itinerant magnetism [21–24]. Besides quantifying the temperature-dependent average magnetization and spin-correlation functions, these works have revealed important qualitative differences between the spin fluctuation energies in Fe and Ni nanostructures, which correspond to different types of dominant magnetic excitations: In Fe the fluctuations of the direction of the local moments dominate,

while in Ni the fluctuations of the modulus of the local moments are crucial.

In view of these investigations it would be very interesting to clarify to what extent the magnetic order within the nano-objects and its finite-temperature stability are modified upon deposition on different metallic surfaces. Moreover, one would like to know if the nature of the dominant fluctuations of the local magnetic degrees of freedom changes after deposition. Cluster-substrate hybridizations are likely to affect the effective exchange couplings within the clusters. Metallic surfaces mediate oscillating Ruderman-Kittel-Kasuya-Yosida (RKKY)–like exchange couplings between magnetic adatoms even at relatively long distances [25]. This may lead to competing ferromagnetic (FM) and antiferromagnetic (AF) couplings, either within the cluster, or between the cluster and the substrate, which deserve to be analyzed in some detail. Furthermore, in the case of highly polarizable elements, a significant spin polarization of the surface atoms is induced in the immediate environment of the magnetic adatoms. This has been actually observed in ground-state calculations, for example, in single-layer Fe_N, Co_N, and Ni_N clusters having $N = 1$–7 atoms on Ir(111), Pt(111), and Au(111), and in Co clusters on Pd(111) and Pd(110) [11,26]. Inferring simple trends about the role of these induced moments at finite T is therefore challenging.

The purpose of this paper is to investigate the finite temperature properties of TM magnetic nanostructures on surfaces, by considering small Fe chains, clusters, and a two-dimensional Fe monolayer (ML) on Pt(111) as particularly relevant examples. We consider a many-body d-band Hamiltonian, which is solved by applying a Hubbard-Stratonovich transformation in the static approximation. The details of the theoretical framework are given in Sec. II. A variety of magnetic properties including atom-resolved spin fluctuation energies, average magnetic moments per atom, and spin-correlation functions are discussed in Sec. III. The role of cluster-substrate hybridizations is quantified by comparison with the corresponding results for free clusters having the same structure. Emphasis is given to correlating these results with the specific local and chemical environment of the atoms. Effective exchange interactions between the local magnetic moments are derived by fitting the spin-flip energies predicted by the electronic theory to a phenomenological Ising model including both Fe-Fe and Fe-Pt couplings. In this way the stability of the magnetic order is analyzed from a local perspective taking into account the substrate contributions. Finally, we conclude in Sec. IV with a summary of our main results and an outlook on possible extensions.

II. THEORY

The finite-temperature magnetic properties of Fe nanostructures on Pt(111) are investigated in the framework of the model Hamiltonian

$$\hat{H} = \hat{H}_0 + \hat{H}_I, \tag{1}$$

where the first term

$$\hat{H}_0 = \sum_{l,\alpha,\sigma} \varepsilon_l^0 \, \hat{n}_{l\alpha\sigma} + \sum_{\substack{l \neq m \\ \alpha,\beta,\sigma}} t_{lm}^{\alpha\beta} \, \hat{c}_{l\alpha\sigma}^{\dagger} \hat{c}_{m\beta\sigma} \tag{2}$$

describes the single-particle electronic structure of the valence d electrons in the tight-binding approximation. As usual, $\hat{c}_{l\alpha\sigma}^{\dagger}$, $\hat{c}_{l\alpha\sigma}$, and $\hat{n}_{l\alpha\sigma}$ refer, respectively, to the creation, annihilation, and number operators of an electron with spin σ at the orbital α of atom l. The bare d-level energy of atom l is denoted by ε_l^0, and the hopping integrals between atoms l and m are denoted by $t_{lm}^{\alpha\beta}$. The second term,

$$\hat{H}_I = \sum_l \left[\frac{U_l}{2} \hat{N}_l (\hat{N}_l - 1) - J_l \, \hat{S}_{lz}^2 \right], \tag{3}$$

takes into account the dominant intra-atomic interactions among the d electrons, where

$$\hat{N}_l = \sum_{\alpha} (\hat{n}_{l\alpha\uparrow} + \hat{n}_{l\alpha\downarrow}) \tag{4}$$

is the d-electron number operator at atom l, and

$$\hat{S}_{l_z} = \frac{1}{2} \sum_{\alpha} (\hat{n}_{l\alpha\uparrow} - \hat{n}_{l\alpha\downarrow}) \tag{5}$$

is the z component of the local spin operator. The interaction parameters U_l and J_l entering Eq. (3) are the average direct and exchange Coulomb integrals, which are specific to the Fe and Pt atoms. Details on the derivation of the model interaction $\hat{H}_I$ may be found in Ref. [9]. It should be however noted that the model given by Eq. (3) does not respect spin-rotational symmetry, since the exchange terms of the form $\hat{H}_{xy} = -\sum_{l,\alpha<\beta} J_l^{\alpha\beta} (\hat{S}_{l\alpha}^{-} \hat{S}_{l\beta}^{+} + \hat{S}_{l\alpha}^{+} \hat{S}_{l\beta}^{-})$ have been dropped [9,27]. This is not expected to be a serious limitation in the present work, since we are interested in studying the effects of SFs on broken-symmetry FM ground states. The perspectives of improving the model will be discussed in Sec. IV. Finally, with an appropriate redefinition of the single-particle d levels ε_l^0 (i.e., $\varepsilon_l^0 \to \varepsilon_l^0 + U_l/2$) one may write the interaction term as

$$\hat{H}_I = \sum_l \left(\frac{U_l}{2} \hat{N}_l^2 - J_l \, \hat{S}_{lz}^2 \right). \tag{6}$$

The thus obtained sum of squares of operators is suitable for applying the Hubbard-Stratonovich transformation and the resulting functional-integral approach [28–30].

The finite-temperature magnetic properties of clusters on Pt(111) are derived from the grand canonical partition function

$$Z = \mathrm{Tr}\,[e^{-\beta(\hat{H} - \mu \hat{N})}], \tag{7}$$

where $\beta = 1/k_{\mathrm{B}} T$, μ refers to the chemical potential, and

$$\hat{N} = \sum_{l,\alpha} (\hat{n}_{l\alpha\uparrow} + \hat{n}_{l\alpha\downarrow}). \tag{8}$$

Following Ref. [21] we linearize the quadratic terms in Eq. (6) by means of a two-field Hubbard-Stratonovich transformation [31] within the static approximation [27,28]. A charge field η_l and an exchange field ξ_l are introduced at each site l, which represent the local finite-temperature fluctuations of the d-electron energy levels and exchange splittings, respectively. Using the notation $\vec{\xi} = (\xi_1, \ldots, \xi_N)$ and $\vec{\eta} = (\eta_1, \ldots, \eta_N)$ for an N-sites system, one obtains [28,31]

$$Z \propto \int e^{-\beta F'(\vec{\xi},\vec{\eta})} d\vec{\eta} \, d\vec{\xi}, \tag{9}$$

where the grand canonical potential or free energy associated to the charge and exchange fields $\vec{\eta}$ and $\vec{\xi}$ is given by

$$F'(\vec{\xi},\vec{\eta}) = \frac{1}{2}\sum_l \left(U_l\,\eta_l^2 + \frac{J_l}{2}\xi_l^2\right) - \frac{1}{\beta}\ln\{\mathrm{Tr}[e^{-\beta(\hat{H}'-\mu\,\hat{N})}]\}. \tag{10}$$

The effective Hamiltonian

$$\hat{H}' = \sum_{l,\alpha,\sigma} \varepsilon'_{l\sigma}\,\hat{n}_{l\alpha\sigma} + \sum_{\substack{l\neq m\\ \alpha,\beta,\sigma}} t_{lm}^{\alpha\beta}\,\hat{c}^{\dagger}_{l\alpha\sigma}\hat{c}_{m\beta\sigma}, \tag{11}$$

describes the dynamics of the d electrons as if they were independent particles moving in a random alloy with energy levels $\varepsilon'_{l\sigma}$ given by

$$\varepsilon'_{l\sigma} = \varepsilon_l^0 + U\,i\,\eta_l - \sigma\frac{J}{2}\xi_l. \tag{12}$$

The thermodynamic properties of the system are obtained as a statistical average over all possible distributions of the energy levels $\varepsilon'_{l\sigma}$ throughout the cluster and its environment. The present static approximation is exact in the atomic limit ($t_{lm}^{\alpha\beta} = 0$, $\forall l \neq m$) where no charge fluctuations are present, and in the noninteracting limit ($U_l = J_l = 0$).

In the low-temperature limit, the dominant field configurations correspond to the saddle point in F'. From Eqs. (10)–(12) one obtains

$$\frac{\partial F'(\vec{\xi},\vec{\eta})}{\partial \xi_l} = \frac{J_l}{2}(\xi_l - 2\langle\hat{S}_{lz}\rangle') \tag{13}$$

and

$$\frac{\partial F'(\vec{\xi},\vec{\eta})}{\partial \eta_l} = U_l(\eta_l + i\,\langle\hat{N}_l\rangle'), \tag{14}$$

where

$$\langle\hat{N}_l\rangle' = \sum_{\alpha,\sigma}\int_{-\infty}^{+\infty}\rho_{l\alpha\sigma}(\varepsilon)\,f(\varepsilon)\,d\varepsilon \tag{15}$$

and

$$2\langle\hat{S}_l\rangle' = \sum_{\alpha,\sigma}\sigma\int_{-\infty}^{+\infty}\rho_{l\alpha\sigma}(\varepsilon)\,f(\varepsilon)\,d\varepsilon. \tag{16}$$

Here, $\langle\ldots\rangle'$ indicates average with respect to the single-particle Hamiltonian H', which depends on $\vec{\xi}$ and $\vec{\eta}$, $f(\varepsilon)$ is the Fermi function, and $\rho_{l\alpha\sigma}(\varepsilon)$ is the local density of states (DOS) at the orbital $l\alpha\sigma$ [21]. In Eq. (16) $\sigma = 1$ ($\sigma = -1$) corresponds to spin up (down). Notice that by setting Eqs. (13) and (14) equal to zero one recovers the usual self-consistent mean-field equations for η_l and ξ_l at $T = 0$ [13]. The present formulation is therefore a natural finite-temperature extension of a widely used ground-state mean-field approach [13–16,26].

Since we are mainly interested in the magnetic properties, and since $J_l \ll U_l$, we neglect the thermal fluctuations of the charge fields η_l by setting them equal to the saddle-point values $\overline{\eta}_l = -i\,\nu_l = -i\,\langle\hat{N}_l\rangle'$. This amounts to a self-consistent determination of the charge distribution for each exchange-field configuration $\vec{\xi}$. Since the average local occupations ν_l are implicit functions of $\vec{\xi}$, one may write

$$Z \propto \int e^{-\beta F'(\vec{\xi})}\,d\vec{\xi}, \tag{17}$$

where

$$F'(\vec{\xi}) = -\frac{1}{2}\sum_l\left(U_l\,\nu_l^2 - \frac{J_l}{2}\xi_l^2\right) - \frac{1}{\beta}\ln\{\mathrm{Tr}[e^{-\beta(\hat{H}'-\mu\,\hat{N})}]\} \tag{18}$$

represents the free energy associated to the exchange-field configuration $\vec{\xi}$, describing the relevant fluctuations of the spin degrees of freedom. Notice that $F'(\vec{\xi})$ in Eqs. (17) and (18) is actually a shorthand for $F'(\vec{\xi},\vec{\eta}(\vec{\xi}))$, where $\vec{\eta}$ refers to the saddle-point value of $\vec{\eta}$ for the exchange-field configuration $\vec{\xi}$. The integrand in Eq. (17) is proportional to the joint probability-density distribution $P(\vec{\xi})$ of the exchange variable $\vec{\xi}$.

The thermodynamic properties are obtained by averaging over all possible $\vec{\xi}$ with $\exp\{-\beta F(\vec{\xi})\}$ as weighting factor. For example, the local magnetization at atom l is given by

$$\begin{aligned} m_l(T) &= \frac{1}{Z}\int e^{(\beta/2)\sum_l(U_l\,\nu_l^2-(J_l/2)\xi_l^2)}\,\mathrm{Tr}\left[2\hat{S}_l^z\,e^{-\beta(\hat{H}'-\mu\hat{N})}\right]d\vec{\xi}\\ &= \frac{1}{Z}\int 2\langle S_{lz}\rangle'\,e^{-\beta F'(\vec{\xi})}\,d\vec{\xi}, \end{aligned} \tag{19}$$

where $\langle S_{lz}\rangle'$ is the average spin moment corresponding to the effective single-particle Hamiltonian $\hat{H}'$, which depends on the fluctuating $\vec{\xi}$. Integrating Eq. (19) by parts, by taking into account Eq. (13) and the saddle-point condition on ν_l, one obtains

$$m_l(T) = \int \xi\;P_l(\xi)\,d\xi, \tag{20}$$

where we have introduced the probability

$$\begin{aligned} P_l(\xi) &= \frac{1}{Z}\,e^{-\beta F'_l(\xi)}\\ &= \frac{1}{Z}\int e^{-\beta F'(\xi_1,\ldots,\xi_{l-1},\xi,\xi_{l+1},\ldots,\xi_N)}\prod_{m\neq l}d\xi_m \end{aligned} \tag{21}$$

that the exchange field at atom l takes the value ξ. Notice, that the temperature-dependent local free energy $F'_l(\xi)$ is obtained by averaging over all possible values of ξ_m for $m \neq l$. Equation (20) shows that the temperature-dependent local magnetization is equal to the average of the local exchange field. This justifies the intuitive association between the fluctuations of the local moment $2\langle\hat{S}_{lz}\rangle$ at atom l and those of the exchange field ξ_l.

In the case of finite clusters no preferred or remanent direction of the magnetization is imposed by the substrate. Therefore, a restriction $\sum_l \xi_l \geqslant 0$ must be enforced in Eq. (20) in order to avoid trivially vanishing results for $m_l(T)$ due to time-inversion symmetry [23]. In this case we compute the z component of the local spin magnetization at atom l from

$$m_l(T) = \frac{1}{Z}\int \mathrm{sgn}\left(\sum_{l=1}^{N}\xi_l\right)\xi_l\,e^{-\beta F'(\vec{\xi})}\,d\vec{\xi}, \tag{22}$$

where the summation runs over the atoms l of the Fe_N cluster. The total cluster magnetization per atom is given by

$$\overline{m}_N(T) = \frac{1}{N}\sum_{l=1}^{N} m_l(T). \tag{23}$$

A first insight on the stability of the magnetic order within the deposited nanostructures is given by the low-temperature limit of $F_l'(\xi)$. In this case, the integration in Eq. (21) can be simplified by setting ξ_m equal to the corresponding ground-state value $\xi_m^0 = \mu_m^0$ for $m \neq l$. In this context, it is useful to introduce the local SF energy

$$\Delta F_l'(\xi) = F_l'(\xi) - F_l'\left(\xi_l^0\right), \tag{24}$$

where $\xi_l^0 = \mu_l^0$ is the local moment of atom l at $T = 0$. $\Delta F_l'(\xi)$ represents the energy involved in an exchange-field (XF) fluctuation at atom l above the ground-state configuration $\vec{\xi}^{\,0}$. Since $\Delta F_l'(\xi)$ determines the probability of the fluctuation $\Delta\xi_l = \xi_l - \xi_l^0$ under the constraint $\xi_m = \xi_m^0$ for all $m \neq l$, it allows us to infer the stability of the ground-state magnetic order at low T.

In order to quantify the short-range order between the local magnetic moments we consider the spin correlation functions

$$\gamma_{lk} = 4\langle \hat{S}_{lz}\, \hat{S}_{kz}\rangle = -\frac{2}{\beta J}\,\delta_{lk} + \frac{1}{Z}\int \xi_l\, \xi_k\, e^{-\beta F'(\vec{\xi})}\, d\vec{\xi}, \tag{25}$$

where the indices l and k refer to the different Fe or Pt atoms. Positive (negative) values of γ_{lk} indicate FM (AF) correlations. The last equality is obtained by successive partial integrations, using Eq. (13) and the saddle-point condition on ν_l. For $l = k$, Eq. (25) gives the local magnetic moment

$$\mu_l = 2\sqrt{\langle \hat{S}_{lz}^2\rangle} = \sqrt{\gamma_{ll}}. \tag{26}$$

As in the case of m_l, γ_{lk} and μ_l are given by a statistical average over the probability density distribution $P(\vec{\xi})$. In addition, Eq. (25) allows us to derive complementary information on the average cluster magnetization per atom by calculating

$$\overline{\mu}_N(T) = \frac{2}{N}\sqrt{\langle \hat{S}_z^2\rangle}, \tag{27}$$

where

$$4\langle \hat{S}_z^2\rangle = \sum_{lk}\gamma_{lk} = -\frac{2N}{\beta J} + \frac{1}{Z}\int \xi^2\, e^{-\beta F'(\vec{\xi})}\, d\vec{\xi}, \tag{28}$$

and $\xi^2 = (\sum_l \xi_l)^2$. Equation (28) shows that there are two main reasons for the decrease of $\overline{\mu}_N(T)$ with increasing T. On the one side, one should analyze how the temperature induced electronic excitations affect the stability of the local magnetic moments $\mu_l = \sqrt{\gamma_{ll}}$. And, on the other side, one should follow the stability of the magnetic order within the nanostructure as given by γ_{lk} for $l \neq k$.

III. RESULTS

In this section we present and discuss results for Fe chains, clusters, and a monolayer deposited on Pt(111). Epitaxial growth is assumed, so that the NN distance between the Fe adatoms corresponds to Pt [$d_{\mathrm{NN}}(\mathrm{Pt}) = 2.77$ Å]. The parameters used for the calculations are the following. The Fe d-band filling $n_d = 6.8$ is derived from spd-band calculations [32]. For Fe the average direct Coulomb integral $U_{\mathrm{Fe}} = 6.0$ eV and the exchange integral $J_{\mathrm{Fe}} = 0.7$ eV yield the experimental bulk magnetization at $T = 0$. In the case of Pt, $U_{\mathrm{Pt}} = 5.9$ eV is taken from atomic calculations and the exchange integral $J_{\mathrm{Pt}} = 0.7$ eV is obtained from local spin-density calculations [33,34].

A. Fe chains on Pt(111)

In the following we consider finite one-dimensional (1D) Fe_N chains on Pt(111) including the 1D limit. For the sake of comparison, results are also given for the free-standing Fe_7 chain having the same NN distance as the deposited ones. Despite a significant hybridization between the deposited chains and the substrate, we observe that the ground-state local magnetic moments μ_l^0 at the Fe atoms are very similar to those found in free-standing chains. For free Fe chains having $N =$ 2–9 atoms and Pt-bulk NN distances we find $\mu_l^0 \simeq 3.2\mu_{\mathrm{B}}$, while in the case of deposited chains we obtain a somewhat smaller $\mu_l^0 \simeq 3.15\mu_{\mathrm{B}}$. These small differences can be ascribed to the cluster-substrate hybridizations, which broaden the discrete cluster density of states, and to the small exchange splittings at the Pt atoms near the chain, which tend to reduce the spin polarization at the Fe atoms. We have verified that these trends remain qualitatively unchanged when sp electrons and spd hybridizations are explicitly taken into account. Moreover, the ground-state moments are weakly affected by reasonable changes in the interatomic distances within the Fe chains. If the NN distances d_{NN} within free-standing Fe chains are allowed to relax, an important contraction is obtained. For example, density-functional calculations based on a generalized gradient approximation to exchange and correlation yield $d_{\mathrm{NN}} = 2.25$–2.27 Å [35–37]. However, the corresponding ground-state moments $\mu_l^0 \simeq 3.1\mu_{\mathrm{B}}$ do not change significantly. This is the consequence of the extremely low dimensionality of the 1D chains, which tends to stabilize saturated local moments.

Small magnetic moments are induced at the Pt atoms in the immediate vicinity of the Fe chains. In the case of a single adatom we find $\mu_{\mathrm{Pt}}^0 = 0.2\mu_{\mathrm{B}}$ at the NN Pt atoms. Moreover, an interesting environment dependence of μ_{Pt} is observed as the chain length grows. Pt atoms having two NN Fe atoms show $\mu_{\mathrm{Pt}}^0 = 0.3\mu_{\mathrm{B}}$ while Pt atoms having only one NN Fe atom show a smaller $\mu_{\mathrm{Pt}}^0 = 0.16$–$0.2\mu_{\mathrm{B}}$. This magnetic proximity effect concerns not only the Pt-Fe bonds but also the Pt-Pt bonds, since Pt atoms having Pt neighbors with significant local magnetic moments develop larger μ_{Pt}^0 than those having only very weakly polarized Pt neighbors. It would be interesting to experimentally determine the Pt contributions to the magnetization of these nanostructures.

The low-temperature limit of the local SF energies $\Delta F_l'(\xi)$ shown in Fig. 1 provides us with an important insight on the stability of the FM order in linear Fe chains on Pt(111). $\Delta F_l'(\xi)$ shows a double-well shape as a function of ξ, with two local minima at $\xi = \mu_l^0$ and $\xi \simeq -\mu_l^0$, where μ_l^0 refers to the ground-state Fe moment. This behavior is characteristic of Fe, where the changes in the exchange energy $\Delta E_X = -J\mu_l^2/4$ associated to the SFs dominate over the changes in the kinetic or band energy ΔE_K. This also explains the strong stability of

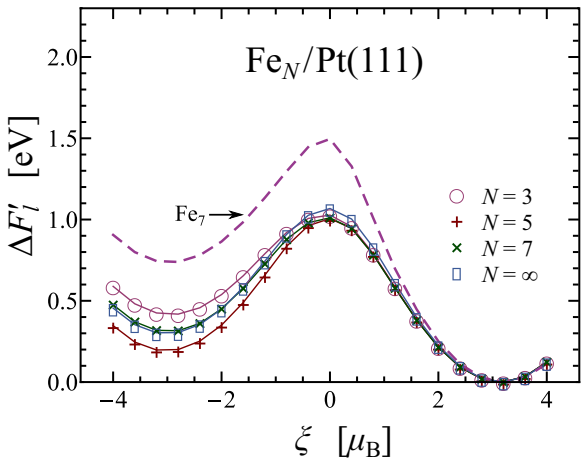

FIG. 1. Low-temperature limit of the local spin-fluctuation energy $\Delta F_l'(\xi)$ as a function of the exchange field (XF) ξ at the central atom of Fe$_N$ linear chains deposited on Pt(111). All other XFs remain fixed to their corresponding ground-state values [see Eq. (24)]. The dashed curve shows $\Delta F_l'(\xi)$ at the central atom of a free-standing Fe$_7$ linear chain.

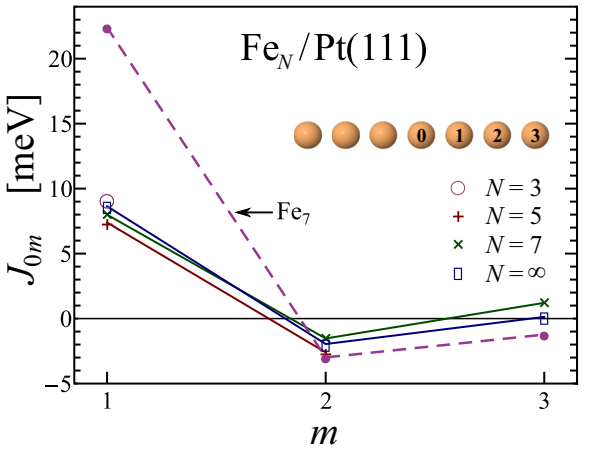

FIG. 2. Effective exchange coupling constants J_{0m} in Fe$_N$ chains on Pt(111) between the central atom $l=0$ and its mth NN. For comparison, results are also given for the free-standing Fe$_7$ chain (dashed line). The lines connecting the points are a guide to the eye.

the local Fe moments at finite T. Notice that ΔE_X does not change upon reversing the local XF from $\xi_l \simeq \mu_l^0$ to $\xi_l = -\mu_l^0$. In contrast, a reduction of ξ_l implies an important increase of ΔE_X, of the order $J(\mu_l^0)^2/4 \simeq 1.74$ eV for $\xi_l \simeq 0$. The difference between the purely exchange energy ΔE_X and the actual spin-fluctuation energy $\Delta F_l'(\xi)$, shown in Fig. 1, reflects the kinetic- or band-energy contribution ΔE_K of the itinerant d electrons. In fact, only in the atomic limit (vanishing hoppings) one has $\Delta F_l'(\xi) = J(|\xi| - \mu_l^0)^2/4$, which corresponds to two degenerate local minima at $\xi = \pm\mu^0$. In 1D systems, the low local coordination number tends to reduce the band energy and its fluctuations, while μ_l^0 and ΔE_X, being local properties, are much less affected. We conclude that the dominant magnetic excitations in Fe chains on Pt(111) are fluctuations of the orientations of the local moments, keeping their size nearly constant. Qualitatively, the same behavior is found in the free-standing case [21], as illustrated by the results for linear Fe$_7$ shown in Fig. 1. The situation is, however, different when the local ground-state moments are small. As we shall see, at the Pt atoms near the deposited cluster, the fluctuations of the size of the local moments dominate over the spin flips.

Taking into account the diversity of experimental routes to magnetic nanostructures (e.g., free-cluster beams, cluster-beam deposition, diffusion-controlled aggregation, etc.) [12] it is most interesting to quantify the effects of the environment on the spin-fluctuation energies. Despite qualitative similarities, the quantitative differences between $\Delta F_l'$ in free-standing and deposited Fe chains are significant. One observes that upon deposition the spin-flip energies $\Delta F_l'(-\xi^0)$ are reduced by about 50%. This implies that reversing a local magnetic moment in the deposited chain involves a much smaller increase of the band energy ΔE_K than in the free-standing geometry. In addition, the energy barrier $\Delta F_l'(\xi = 0)$ between the minima is reduced by about 30%. Consequently, deposition leads to flatter energy landscapes, as compared to the free-standing case, which weakens the stability of FM order at finite temperatures. We conclude that the hybridizations between the magnetic clusters and the nonmagnetic or weakly magnetic Pt substrate have a stronger effect on the magnetic excitations than on the ground-state spin-polarized density distribution.

It is interesting to note that the spin-flip energy $\Delta F_l'(-\xi^0)$ shown in Fig. 1 oscillates as a function of chain length, approaching closely the infinite length limit already for $N \simeq$ 7–10 atoms. An analogous behavior has been observed in the case of free-standing chains and clusters [23]. This suggests the possible presence of competing FM and AF couplings between the Fe local moments at different distances within the chain. In order to examine this problem in more detail, we have determined the effective exchange coupling constants J_{0m} between the central atom of the chain and its mth NN in the framework of a classical Ising model. All possible orientations of the local XFs ξ_l within the chain are considered, by keeping their absolute values equal to the corresponding ground-state moments μ_l^0. In Fig. 2 results are given for J_{0m} between the local moment at the central atom, $l=0$, and its mth NN in Fe$_N$ chains on Pt(111). As expected, the NN exchange couplings J_{01} are positive and largest. In contrast, the second NN couplings J_{02} are significantly smaller and negative. For larger distances J_{0m} oscillates as a function of m showing rapidly decreasing absolute values. Although free-standing chains show a qualitatively comparable dependence of J_{0m} as a function of m, the quantitative differences are most significant. In particular, the NN coupling constants are about two times larger in the free-standing chains than in the deposited ones. Similar oscillations of the effective exchange coupling constants have been obtained in first-principles calculations on infinite TM chains [36–39].

B. Fe clusters on Pt(111)

In this section we investigate the properties of deposited Fe clusters, whose structures and local environments are illustrated in Fig. 3. The corresponding SF energies $\Delta F_l'(\xi)$ of Fe$_N$ and of the infinite 2D ML deposited on Pt(111) are shown in Figs. 4 and 5. For the sake of comparison, results are

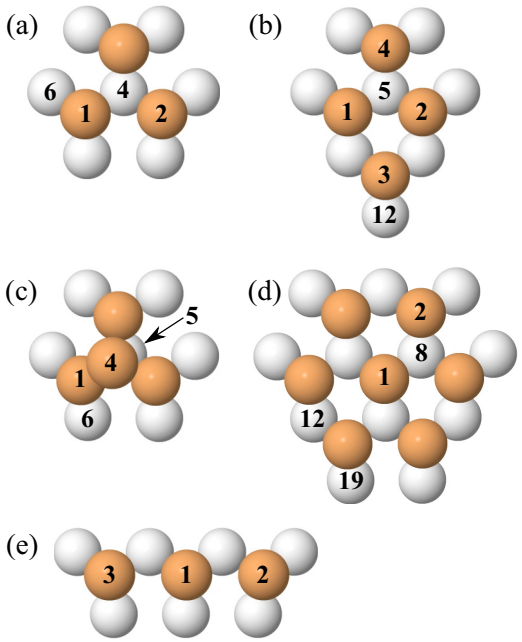

FIG. 3. Illustration of the considered Fe_N clusters on Pt(111). Dark (light) spheres indicate Fe (Pt) atoms. The numbers label the different sites l.

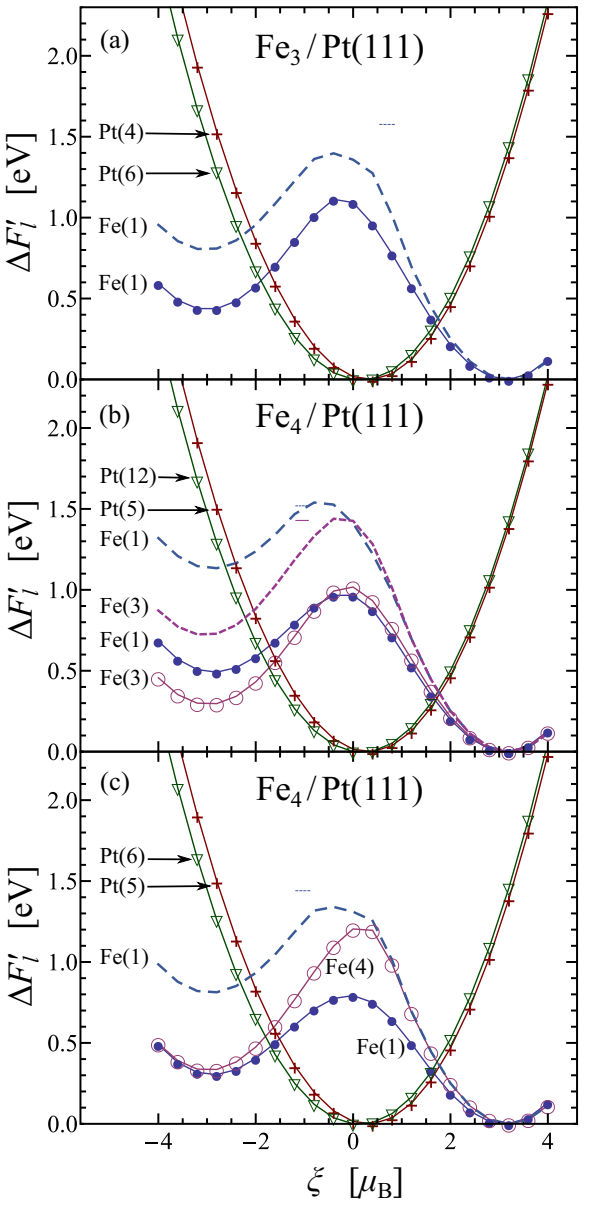

FIG. 4. Local SF energy $\Delta F_l'(\xi) = F_l'(\xi) - F_l'(\xi^0)$ at the different Fe and Pt atoms l of Fe_N clusters deposited on Pt(111): (a) triangle, (b) rhombus, and (c) tetrahedron. The cluster structures together with the atom labels are illustrated in Fig. 3. The dashed curves correspond to free-standing Fe_N clusters having the same structure and bond lengths as the deposited ones.

also given for free-standing clusters having the same structure and bond lengths. Concerning the ground state, one obtains FM order with nearly saturated local magnetic moments $\mu_l^0 \simeq 3.1$–$3.2\mu_B$ at the Fe atoms. Small induced local magnetic moments $\mu_{Pt}^0 \simeq 0.13$–$0.32\mu_B$ are found at the Pt atoms in the vicinity of Fe_N. As in the finite chains, $\Delta F_l'(\xi)$ at the Fe atoms shows two local minima at $\xi = \mu_l^0$ and $\xi \simeq -\mu_l^0$. This confirms the expected dominant role of spin-flip excitations at the Fe atoms, in qualitative agreement with the results for free-standing Fe clusters and ML reported in Refs. [21,22]. Nevertheless, deposition changes the SF energy landscapes quantitatively. Comparison with free clusters having the same Pt bulk NN distances shows that the spin-flip energy $\Delta F_l'(-\xi^0)$ is actually reduced by about 50% upon deposition on Pt(111). In the case of the hexagonal Fe_7, $\Delta F_l'(-\xi^0)$ at the central and outer atoms are reduced to only 30% of the free-cluster value. In other clusters, or in the 2D ML, the effects of hybridization with the substrate are less strong, though still significant (see Figs. 4 and 5). As in linear Fe_N, deposition on Pt(111) renders the SF energy landscapes flatter, thus weakening the stability of FM order at finite temperatures.

In contrast to the Fe atoms, the Pt atoms near the Fe cluster or at the interface with the Fe ML show only one local minimum in $\Delta F_l'(\xi)$. In the low-temperature limit this is located at the small induced ground-state magnetic moment μ_l^0. $\Delta F_l'(\xi)$ takes here a paraboliclike form with a slight asymmetry favoring XF fluctuations towards smaller exchange splittings (i.e., $\xi < \mu_{Pt}^0$). Thus, $\mu_{Pt}(T)$ decreases with increasing T. Clearly, the fluctuations of the size of the local magnetic moments are dominant here. Notice that the precise position of the minimum in $\Delta F_l'(\xi)$ depends on the local chemical environment of the Pt atoms, since it follows the environment dependence of the ground-state moments μ_l^0. For example, in the triangular Fe_3 on Pt(111) we find $\mu_4^0 = 0.33\mu_B$ at the Pt atom $l = 4$, which has three NN Fe atoms. This is twice as large as the local moment $\mu_6^0 = 0.16\mu_B$ found at the $l = 6$ Pt atom, which has only one NN Fe atom (see Fig. 3).

An interesting environment dependence is also observed in the tetrahedral Fe_4. While μ_l^0 at the Fe-Pt interface is reduced to $\mu_1^0 = 3.11\mu_B$, the topmost Fe atom $l = 4$ shows $\mu_4^0 = 3.196\mu_B$, which is very close to the free-standing value $\mu_4^0 = 3.197\mu_B$. This is consistent with the low local coordination of this atom and the weaker influence of the more distant Pt surface. However, the changes in the spin-flip energy $\Delta F_l'(-\xi^0)$ upon deposition are much more significant.

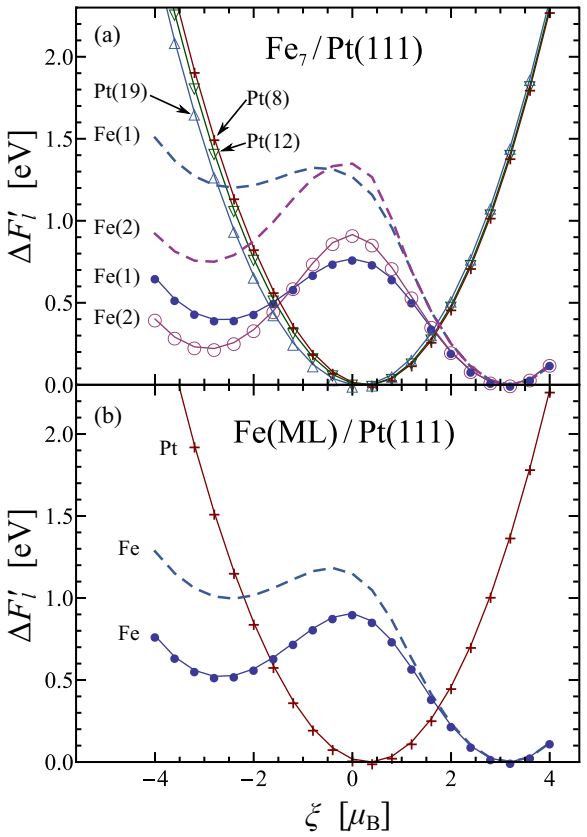

FIG. 5. Local SF energy $\Delta F_l'(\xi)$ at the different Fe and Pt atoms l of (a) a hexagonal Fe_7 cluster and (b) the Fe (ML) deposited on Pt(111) (see Fig. 3). Results for the corresponding free-standing configurations are shown by the dashed curves.

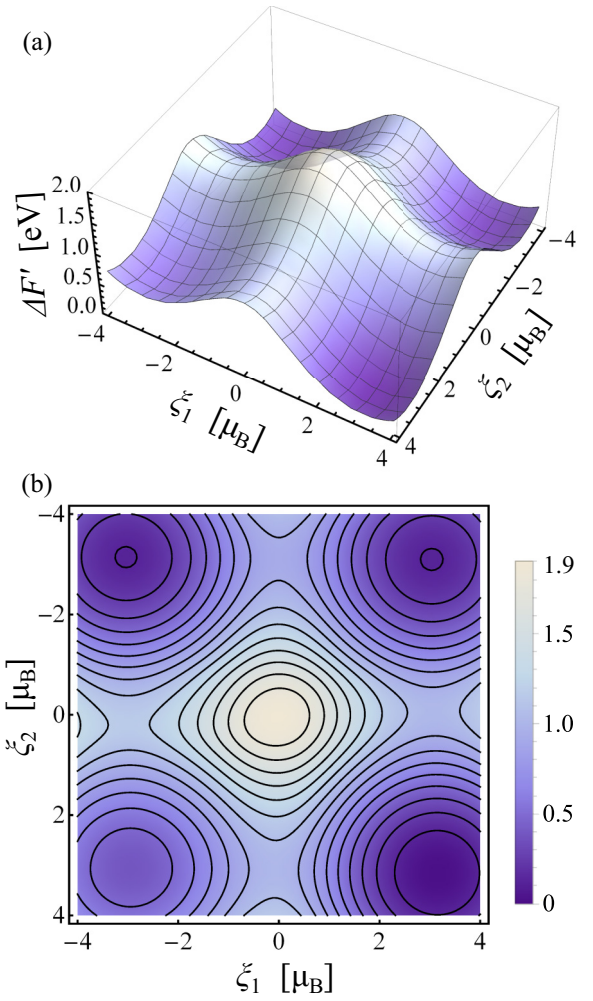

FIG. 6. Spin-fluctuation energy landscape of linear Fe_3 deposited on Pt(111). In (a) $\Delta F'(\xi_1,\xi_2) = F'(\xi_1,\xi_2,\xi_3^0) - F'(\xi_1^0,\xi_2^0,\xi_3^0)$ is given as a function of the XFs ξ_1 and ξ_2 at the central atom and at an edge atom [see Fig. 3(e)]. In (b) the corresponding contour plot is shown. The XFs at the other edge Fe atom ($l = 3$) and at the Pt substrate are kept equal to their ground-state values.

Indeed, as shown in Fig. 4, $\Delta F_l'(-\xi^0)$ is reduced upon deposition by approximately 50% at all Fe atoms. This can be understood by recalling that in TMs the magnetic degrees of freedom and their couplings originate from delocalized itinerant-electron states. Therefore, the magnetic excitations and the resulting finite-temperature properties depend on the local environment at a broader distance range. At least in this case, cluster-substrate hybridizations affect the couplings between the local moments, and the stability of the magnetic order, much more strongly than the low-temperature local moments. Thus, the consequences of cluster deposition are more significant at finite temperatures.

C. Temperature dependence

In the following we consider small Fe_N clusters deposited on Pt(111) with $N = 3$ and 4 atoms. In order to obtain the equilibrium properties at finite T, we average over all possible XF configurations $\vec{\xi}$ taking into account that the probability $P(\vec{\xi})$ for the field configuration $\vec{\xi}$ is proportional to $\exp\{-\beta F'(\vec{\xi})\}$ [see Eqs. (20), (21), and (25)]. In order to illustrate the coupling between spin fluctuations at different atoms, we show in Fig. 6 results for $F'(\vec{\xi})$ in linear Fe_3 on Pt(111) as a function of the XFs ξ_1 and ξ_2 at the central atom and at an edge atom. For simplicity, all other XFs are kept fixed to the corresponding ground-state values ξ_l^0. One may first notice the four local minima located approximately at $(\xi_1,\xi_2) = (\pm\xi_1^0, \pm\xi_2^0)$. The transition states connecting them correspond to a vanishing XF, keeping the other one close to $\pm\mu_l^0$. As expected, the paramagnetic configuration having $\vec{\xi} = 0$ yields the maximum in the energy landscape. Qualitatively, the overall shape of the energy landscape can be understood by recalling the dominant role played by exchange energy ΔE_X in the case of strong local magnetic moments.

In Fig. 7 results are given for the temperature dependence of the average magnetic moment per atom $\overline{\mu}_N$ of the triangular Fe_3, linear Fe_3, and rhombohedral Fe_4 deposited on Pt(111). Starting from the nearly saturated ground-state value, $\overline{\mu}_N$ decreases with increasing T in a qualitatively similar way as in free clusters [23]. Thus, the stability of FM order within the clusters, which has already been observed in the gas phase, is preserved upon deposition. Concerning the dependence on size and structure, one finds that $\overline{\mu}_N(T)$ is always larger in the triangle than in the rhombus, which in turn has a larger $\overline{\mu}_N(T)$ than in the linear trimer. This trend can be qualitatively

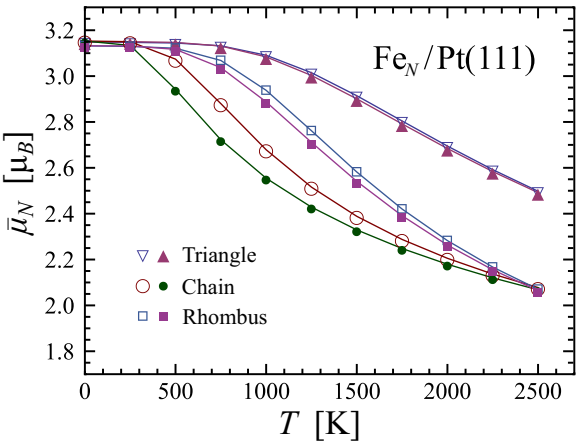

FIG. 7. Temperature dependence of the average magnetic moment per atom $\overline{\mu}_N$, given by Eq. (27), for the triangular Fe_3 (triangles), linear Fe_3 (circles), and rhombohedral Fe_4 (squares) on Pt(111) (see Fig. 3). The XFs ξ at the Pt atoms are either fixed to the ground-state values (open symbols) or computed self-consistently (full symbols) for each XF configuration of the Fe cluster.

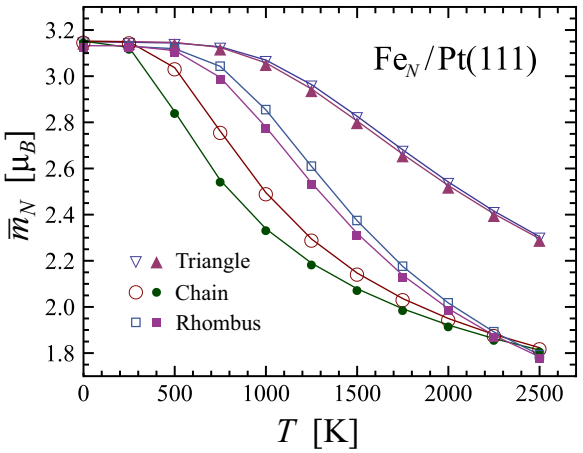

FIG. 8. Temperature dependence of the average magnetization per atom $\overline{m}_N$, given by Eq. (23), for triangular Fe_3 (triangles), linear Fe_3 (circles), and rhombohedral Fe_4 (squares) on Pt(111). The XFs at the Pt atoms are either fixed to the ground-state values (open symbols) or calculated self-consistently for each XF configuration of the Fe cluster (full symbols).

understood by comparing the local environments of the atoms in the different clusters, taking into account the competing effective exchange couplings J_{lm} between the local moments. Let us recall that J_{01} between NNs was found to be strongly FM, while J_{02} between second NNs is weakly AF. The strong decrease of $\overline{\mu}_N(T)$ in linear Fe_3, as compared to the triangle, can be regarded as the consequence of replacing a strong FM first-NN coupling by a weaker AF second-NN coupling. In the case of the rhombus, the decrease of $\overline{\mu}_N$ with increasing T is triggered by the lowest coordinated atoms [$l = 3$ and $l = 4$ in Fig. 3(b)]. Although these atoms have the same number of first NNs as in the triangle, the additional AF second-NN coupling lowers the local SF energy, thereby reducing the stability of FM order. This interpretation is consistent with results for the spin-correlation functions γ_{lm} to be discussed below.

A qualitative measure of the stability of ferromagnetism in small clusters is provided by the inflection point in $\overline{\mu}_N(T)$, which can be interpreted as a precursor of the thermodynamic phase-transition temperature or cluster Curie temperature $T_C(N)$. For the deposited Fe_3 chain we find $T_C(N) \simeq 750$ K, for the rhombus $T_C(N) \simeq 1400$ K, and for the triangle $T_C(N) \simeq 2200$ K. In the high-temperature limit, where $k_B T$ is much larger than the effective exchange couplings $J_{0m} \sim 10^3$ K but still smaller than the d-band exchange splitting $\Delta E_X \sim 10^4$ K, we observe that $\overline{\mu}_N(T)$ tends approximately to $\overline{\mu}_N(T = 0)/\sqrt{N}$. This corresponds to the average of N randomly oriented local magnetic moments having approximately the same length as the ground-state local moments [40]. In the case of the linear trimer $\overline{\mu}_3(T = 2500\ \text{K})$ is in fact not very far from $\overline{\mu}_3(T = 0)/\sqrt{3} \simeq 1.8\mu_B$.

Comparing our results for $\overline{\mu}_N(T)$ of Fe_N on Pt(111) with those of free clusters having the same structures and NN distances, one concludes that the hybridization with the substrate reduces significantly the stability of FM order at finite temperatures. For example, in linear Fe_3 we find a decrease of about 50% in $T_C(N)$ upon deposition on Pt(111). This is consistent with the previously discussed reduction of the local SF energies $\Delta F_l'(\xi)$. Similar trends should be observed in experiment when the clusters are deposited on a surface or embedded in a nonmagnetic matrix. Notice, however, that the present comparison does not take into account the consequences of structural relaxations in the free-standing clusters, which are known to modify the temperature dependence of $\overline{\mu}_N$ [23]. Indeed, small Fe clusters have in general shorter equilibrium bond lengths than the Pt bulk NN distance corresponding to epitaxial growth on Pt(111). Such contractions result in an increase of the effective d-band width of free-standing clusters and a reduction of $T_C(N)$. Thus, the effects of hybridization with the nonmagnetic or weakly magnetic substrate may be partially compensated by the changes in bond length and structure occurring in the Fe clusters upon deposition.

An alternative approach to computing the average cluster magnetization is to perform first the thermal average of the local magnetizations $m_l(T)$ independently, according to Eq. (20), and to derive the cluster magnetization $\overline{m}_N(T)$ by averaging $m_l(T)$ according to Eq. (23). Results for $\overline{m}_N(T)$ are shown in Fig. 8 for some representative Fe_N clusters on Pt(111). Comparison with the results for $\overline{\mu}_N(T)$ presented in Fig. 7 shows that both approaches give comparable dependencies on temperature, size, and structure. This is in agreement with previous results for free-standing clusters [23].

In order to assess the effects of the Pt-moment fluctuations on the temperature-dependent magnetic properties, we have performed calculations of $\overline{\mu}_N$ under two extremely opposite assumptions. First, we assume that the exchange splittings at all Pt atoms in the substrate remain equal to their ground-state values μ^0_{Pt}. Such a frozen moment or non-self-consistent (NSC) approach will certainly tend to overestimate $\overline{\mu}_N$ and the stability of FM order within the deposited clusters. Second, we assume that the local XFs at the Pt atoms next to the Fe clusters follow adiabatically the fluctuating Fe moments, so that the energy is minimal for each XF configuration of the latter. Clearly, the adiabatic or self-consistent (SC) approximation

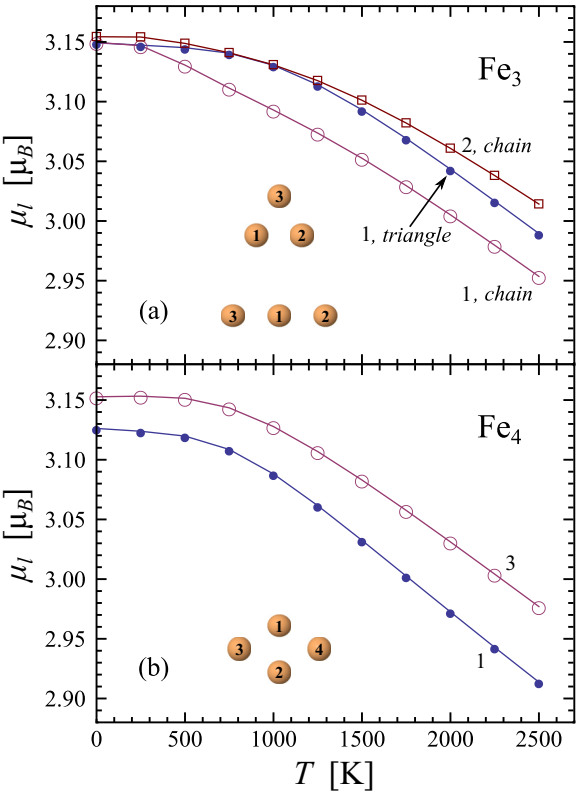

FIG. 9. Temperature dependence of the local magnetic moments $\mu_l = \sqrt{\gamma_{ll}}$ at different atoms l of Fe_N clusters deposited on Pt(111): (a) triangle and chain, and (b) rhombus. The XFs at the Pt atoms are calculated self-consistently (SC) for each XF configuration of the Fe cluster. Assuming fixed ground-state exchange splittings ξ_l^0 at the substrate atoms yields almost the same results.

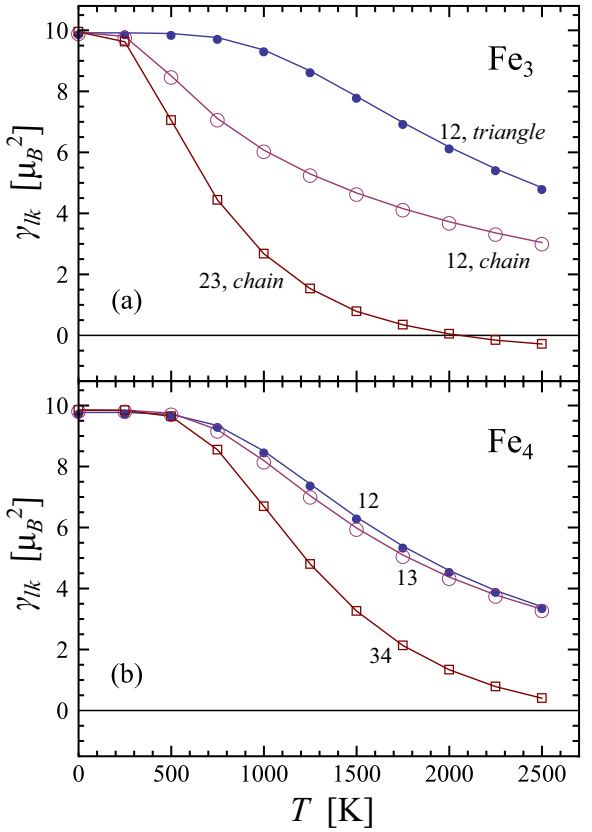

FIG. 10. Temperature dependence of the pair correlation functions γ_{lk} between different atoms l and k of Fe_N clusters deposited on Pt(111): (a) triangle and chain, and (b) rhombus. The cluster structures and atom labeling are shown in the inset of Fig. 9. As in Fig. 9 the results are obtained by treating the XFs at the Pt substrate atoms self-consistently. The NSC approach yields very similar results.

gives a lower bound for the SF energies and should therefore underestimate $\overline{\mu}_N(T)$. Nevertheless, we expect the adiabatic approximation to be physically more relevant, since the local Pt moments are actually induced by the proximity with Fe_N. In Figs. 7 and 8 the two approaches are compared. One concludes that the details of the SFs at the Pt substrate have little influence on the temperature dependence of $\overline{\mu}_N$ and $\overline{m}_N$. The largest effects are found in the linear trimer which, being the most weakly coordinated Fe structure, is more susceptible to the environment. The Fe and Pt contributions to the average magnetization of the nanostructure could be investigated experimentally by means of element-specific x-ray magnetic circular dichroism measurements.

The behavior of $\overline{\mu}_N$ can be analyzed from a local perspective. To this aim we show in Figs. 9 and 10 the local magnetic moments $\mu_l = \sqrt{\gamma_{ll}}$ and the pair-correlation functions γ_{lk} as a function of T. In all cases μ_l remains remarkably stable at finite temperatures. In fact, only a small decrease in μ_l, of about 5%, is observed in the considered temperature range. This is of course understandable, since the stability of the local magnetic moments is controlled by the exchange energy $\Delta E_X = -J\mu_l^2/4$, which is an order of magnitude larger than any reasonable temperature. In the framework of the present functional integral formalism, we can interpret this behavior in terms of the SF energy landscape $\Delta F'(\vec{\xi})$. In Fe systems $\Delta F_l'(\xi)$ shows indeed two deep minima at $\xi \simeq \pm\mu_l^0$. As a result local-moment flips, keeping the absolute value of μ_l approximately constant, are much more probable than reducing the size of the local magnetic moments [i.e., $\Delta F_l'(\xi=0) \gg \Delta F_l'(-\xi^0)$]. One may also point out that μ_l tends to be more stable at the atoms having a smaller local coordination number (see Fig. 9). This is consistent with the localized character of the magnetic excitations at low coordinated sites.

In contrast to μ_l, the pair-correlation functions γ_{lk} $(l \neq k)$ shown in Fig. 10 decrease faster with temperature when the local coordination number is smaller. In particular in linear Fe_3 we have competing FM and AF effective exchange interactions, which tend to weaken the FM order within the chain. The rapid decrease of γ_{23} reflects the resulting rising probability for an antiparallel alignment between local magnetic moments at the edges of the chain. The disorder of the magnetic moments at the edge atoms precludes the local moment at the central atom from having a parallel alignment with both of them. This contributes to a decrease of $\gamma_{12} = \gamma_{13}$ with increasing T.

The results for γ_{lk} in the rhombohedral Fe_4 can be interpreted in an analogous way. In this case the atoms labeled 3 and 4 are also second NNs. As γ_{23} in linear Fe_3, γ_{34} in

the rhombus approaches zero as the temperature increases. In other words, the probabilities for parallel and antiparallel alignment are nearly the same for $T > 2000\ K$. In contrast, the triangle, which has only NN couplings, shows a stronger stability of the correlation functions. It is probably the absence of competing second NN coupling what renders FM order so stable in triangular Fe_3.

IV. CONCLUSION

Iron clusters, linear chains, and a ML deposited on Pt(111) have been investigated in the framework of a functional-integral theory of itinerant magnetism. The consequences of depositing magnetic nano-objects on a highly polarizable nonmagnetic substrate have been quantified by comparison with the corresponding results for free-standing configurations. Finite-size effects have been discussed, including in particular the differences with the infinite 1D Fe chain and the 2D ML on Pt(111). The considered Fe nanostructures are found to have a FM ground state with nearly saturated local magnetic moments μ_l^0. In the case of the Fe atoms the magnetic moments μ_l^0 are somewhat smaller than in free clusters having the same structure and interatomic distances. This can be ascribed to the hybridizations between the cluster electronic states and the broad substrate bands, and to the nonmagnetic character of the bare substrate. At the same time, small local magnetic moments $\mu_{\rm Pt}^0$ are induced at the Pt atoms in the immediate environment of the Fe cluster. The size of $\mu_{\rm Pt}^0 \simeq 0.1$–$0.3\mu_{\rm B}$ depends strongly on the local environment of the Pt atoms: the larger the number of Fe atoms in the NN shell the stronger the induced $\mu_{\rm Pt}^0$.

An important insight on the energy involved in the thermal magnetic excitations and their characteristics has been inferred from the calculated SF energies $\Delta F_l'(\xi)$ at the different Fe and Pt atoms of the nanostructures. At the Fe atoms $\Delta F_l'(\xi)$ shows two local minima located approximately at $\xi = \pm\mu_l^0$. This implies that in Fe the dominant magnetic excitations are flips of the orientation of the local moments keeping their size approximately constant. These trends are in qualitative agreement with previous studies on free-standing chains and clusters [21–23]. However, deposition has a significant impact on the actual spin-flip energies $\Delta F_l'(-\mu_l^0)$ and on the barrier energy $\Delta F_l'(\xi=0)$ separating the minima. In fact, $\Delta F_l'(-\mu_l^0)$ is typically reduced by 50%, while $\Delta F_l'(\xi=0)$ is reduced by about 30%. This leads to significantly flatter SF energy landscapes and, accordingly, to a weaker stability of FM order at finite temperatures. In addition, we have found evidence for competing effective exchange coupling constants J_{lm} between the local Fe moments at different distances within the chains: strong FM couplings J_{01} between NNs and weaker AF couplings J_{02} between second NNs.

The dominant magnetic excitations at the Pt atoms near the cluster have a very different nature. In this case the small induced local moments do not flip significantly; they basically fluctuate in size. The SF energies $\Delta F_l'(\xi)$ at the Pt atoms show a single minimum at $\xi_l^0 = \mu_l^0$ with a slight asymmetry that favors fluctuations of ξ towards values smaller that ξ_l^0. This results in a decrease of the local Pt magnetizations as T increases. It is interesting to observe that such fluctuations of the size of the local moments are characteristic of itinerant ferromagnets with small local moments, such as bulk Ni [21]. They cannot be described in the framework of the phenomenological Heisenberg models that are usually assumed in the context of DFT-based calculations [19,20]. Nevertheless, our results also indicate that the fluctuations of the Pt moments, though present, have little influence on the temperature dependence of the magnetic properties of the deposited Fe clusters.

Finally, we have discussed the temperature dependence of the average magnetization per atom $\overline{\mu}_N$, local magnetic moments μ_l, and spin-correlation function γ_{lk} of small Fe_N clusters on Pt(111). Some qualitative resemblances and important quantitative differences with respect to gas-phase clusters have been identified. An analysis from a local perspective shows that the local magnetic moments μ_l are hardly reduced, by only about 5%, as the temperature increases ($T \leqslant 2500$ K). In contrast, the correlation functions γ_{lk} decrease remarkably fast with increasing T, particularly between second NNs. The decrease of the second NN spin correlations, and the associated spin fluctuations, trigger the decrease of γ_{lk} between first NNs and thus the complete magnetic disorder within the clusters.

The present work extends previous self-consistent tight-binding studies on the ground-state properties of deposited clusters and wires [15,26,41] to finite temperatures. Moreover, it expands the scope of temperature-dependent investigations of the magnetism of small clusters by incorporating substrate effects [21,23]. The results provide a clear insight on the changes in the finite-temperature magnetic behavior, which follow from cluster deposition on highly polarizable substrates. This corresponds to the situation found in many experiments on transition-metal clusters on surfaces, which aim to characterize the local magnetic moments, their couplings, and the stability of the magnetization direction by controlling the size, composition, and local atomic environment [1–6,12]. In addition, a number of interesting perspectives of theoretical improvements and extensions are opened. One central aspect concerns the spin-rotational invariance of the model Hamiltonian and its possible consequences on the ground-state and finite-temperature behavior. Taking into account the competing FM and AF exchange interactions found in this work, one would like to investigate whether this may lead to more complex noncollinear magnetic order in deposited wires, and to what extent they may affect the nature of the dominant spin excitations. In fact, competing magnetic interactions and spiral spin-density-wave instabilities have been observed in the ground state of infinite TM chains [36–39]. Moreover, it would be important to quantify the role of transversal spin fluctuations on the temperature-dependent properties of deposited clusters, chains, and thin films. The comparison between collinear and noncollinear calculations on bulk Fe has recently shown that transversal spin fluctuations become increasingly important with increasing temperature [9]. Taking them into account yields a decrease of about 35% of the Curie temperature predicted for bulk Fe, which amounts to $T_C = 1250$ K and is thus quite close to the experimental value $T_C^{\rm expt} = 1043$ K. Therefore, the calculations reported in this paper are expected to underestimate the magnetic entropy of the deposited nanostructures and overestimate the stability of the magnetic order at finite T. In this context it should be recalled that the available rotational-invariant spin-fluctuation theories of itinerant magnetism in the static approximation fail

in the atomic limit, while the collinear approach considered here is exact [42]. Further theoretical developments in this direction seem worthwhile.

Finally, we would like to comment on the possible role of other contributions to the intra-atomic Coulomb interaction. The basic assumptions behind the derivation of the model Hamiltonian are to focus on the Coulomb interaction among the d electrons within each atom, to neglect the matrix elements which involve more than two different orbitals, and to respect the rotational invariance of the intra-atomic Hamiltonian, which in particular implies the conservation of the orbital angular momentum in electronic collisions [9]. For simplicity, the direct and exchange Coulomb integrals $U_{\alpha\beta}$ and $J_{\alpha\beta}$ are replaced by the element specific average values U_l and J_l. The orbital dependence of Coulomb integrals, but also more involved contributions to the intra-atomic Coulomb interaction [43,44], have been shown to be important for a detailed description of crystal-field splittings, magnetic anisotropy, and orbital magnetism in the ground state [41,44]. This should also hold at finite T, maybe to an even larger extent. However, we do not expect that such a more detailed description of the intra-atomic interactions would have a significant effect on the spin moments and their order, since these contributions involve a much smaller energy scale than the dominant exchange and band energies.

ACKNOWLEDGMENTS

This work has been financed in part by the Deutsche Forschungsgemeinschaft and by the DAAD-CONACyT exchange program PROALMEX. Computer resources provided by the IT Service Center of the University of Kassel and by the Center for Scientific Computing of the University of Frankfurt are gratefully acknowledged.

[1] A. A. Khajetoorians, M. Valentyuk, M. Steinbrecher, T. Schlenk, A. Shick, J. Kolorenc, A. I. Lichtenstein, T. O. Wehling, R. Wiesendanger, and J. Wiebe, Nat. Nanotechnol. **10**, 958 (2015).

[2] K. von Bergmann, Science **349**, 234 (2015).

[3] I. G. Rau, S. Baumann, S. Rusponi, F. Donati, S. Stepanow, L. Gragnaniello, J. Dreiser, C. Piamonteze, F. Nolting, S. Gangopadhyay, O. R. Albertini, R. M. Macfarlane, C. P. Lutz, B. A. Jones, P. Gambardella, A. J. Heinrich, and H. Brune, Science **344**, 988 (2014).

[4] A. Sonntag, J. Hermenau, A. Schlenhoff, J. Friedlein, S. Krause, and R. Wiesendanger, Phys. Rev. Lett. **112**, 017204 (2014).

[5] G. Ju, Y. Peng, E. K. C. Chang, Y. Ding, A. Q. Wu, X. Zhu, Y. Kubota, T. J. Klemmer, H. Amini, L. Gao, Z. Fan, T. Rausch, P. Subedi, M. Ma, S. Kalarickal, C. J. Rea, D. V. Dimitrov, P.-W. Huang, K. Wang, X. Chen, C. Peng, W. Chen, J. W. Dykes, M. A. Seigler, E. C. Gage, R. Chantrell, and J.-U. Thiele, IEEE Trans. Magn. **51**, 3201709 (2015).

[6] F. Donati, Q. Dubout, G. Autes, F. Patthey, F. Calleja, P. Gambardella, O. V. Yazyev, and H. Brune, Phys. Rev. Lett. **111**, 236801 (2013).

[7] I. A. Zhuravlev, V. P. Antropov, and K. D. Belashchenko, Phys. Rev. Lett. **115**, 217201 (2015).

[8] W. Töws and G. M. Pastor, Phys. Rev. B **86**, 054443 (2012).

[9] R. Garibay-Alonso, J. Dorantes-Dávila, and G. M. Pastor, Phys. Rev. B **91**, 184408 (2015).

[10] W. Töws and G. M. Pastor, Phys. Rev. Lett. **115**, 217204 (2015).

[11] S. Bornemann, O. Šipr, S. Mankovsky, S. Polesya, J. B. Staunton, W. Wurth, H. Ebert, and J. Minár, Phys. Rev. B **86**, 104436 (2012).

[12] J. Bansmann, S. H. Baker, C. Binns, J. A. Blackman, J.-P. Bucher, J. Dorantes-Dávila, V. Dupuis, L. Favre, D. Kechrakos, A. Kleibert, K.-H. Meiwes-Broer, G. M. Pastor, A. Perez, O. Toulemonde, K. N. Trohidou, J. Tuaillon, and Y. Xie, Surf. Sci. Rep. **56**, 189 (2005).

[13] G. M. Pastor, J. Dorantes-Dávila, and K. H. Bennemann, Physica B **149**, 22 (1988); Phys. Rev. B **40**, 7642 (1989).

[14] G. M. Pastor, J. Dorantes-Dávila, S. Pick, and H. Dreyssé, Phys. Rev. Lett. **75**, 326 (1995).

[15] J. Dorantes-Dávila and G. M. Pastor, Phys. Rev. Lett. **81**, 208 (1998).

[16] R. A. Guirado-López, J. Dorantes-Dávila, and G. M. Pastor, Phys. Rev. Lett. **90**, 226402 (2003).

[17] J. Dorantes-Dávila, G. M. Pastor, and K. H. Bennemann, Solid State Commun. **59**, 159 (1986); **60**, 465 (1986).

[18] S. Polesya, O. Šipr, S. Bornemann, J. Minár, and H. Ebert, Europhys. Lett. **74**, 1074 (2006).

[19] O. Šipr, S. Polesya, J. Minár, and H. Ebert, J. Phys.: Condens. Matter **19**, 446205 (2007).

[20] O. Šipr, S. Bornemann, J. Minár, S. Polesya, V. Popescu, A. Šimunek, and H. Ebert, J. Phys.: Condens. Matter **19**, 096203 (2007).

[21] G. M. Pastor, J. Dorantes-Dávila, and K. H. Bennemann, Phys. Rev. B **70**, 064420 (2004).

[22] R. Garibay-Alonso, J. Dorantes-Dávila, and G. M. Pastor, Phys. Rev. B **73**, 224429 (2006).

[23] R. Garibay-Alonso, J. Dorantes-Dávila, and G. M. Pastor, Phys. Rev. B **79**, 134401 (2009).

[24] R. Garibay-Alonso, J. Dorantes-Dávila, and G. M. Pastor, Phys. Rev. B **85**, 224409 (2012).

[25] M. A. Rudermann and C. Kittel, Phys. Rev. **96**, 99 (1954); T. Kasuya, Progr. Theor. Phys. **16**, 45 (1956); K. Yosida, Phys. Rev. **106**, 893 (1957).

[26] R. Félix-Medina, J. Dorantes-Dávila, and G. M. Pastor, New J. Phys. **4**, 100 (2002); Phys. Rev. B **67**, 094430 (2003).

[27] B. Mühlschlegel, Z. Phys. **208**, 94 (1968).

[28] J. Hubbard, Phys. Rev. B **19**, 2626 (1979); **20**, 4584 (1979); H. Hasegawa, J. Phys. Soc. Jpn. **49**, 178 (1980); **49**, 963 (1980).

[29] Y. Kakehashi, J. Phys. Soc. Jpn. **50**, 2251 (1981).

[30] *Electron Correlation and Magnetism in Narrow-Band Systems*, Springer Series in Solid State Sciences Vol 29, edited by T. Moriya (Springer, Heidelberg, 1981); D. Vollhardt, N. Blümer, K. Held, M. Kollar, J. Schlipf, M. Ulmke, and J. Wahle, *Advances in Solid State Physics* (Vieweg, Wiesbaden, 1999), Vol. 38, p. 383.

[31] R. L. Stratonovich, Dokl. Akad. Nauk. SSSR **115**, 1097 (1957) [Sov. Phys.-Dokl. **2**, 416 (1958)]; J. Hubbard, Phys. Rev. Lett. **3**, 77 (1959).

[32] D. A. Papaconstantopoulos, *Handbook of the Band Structure of Elemental Solids*, 2nd Ed. (Springer, New York, 2015).
[33] N. E. Christensen, O. Gunnarsson, O. Jepsen, and O. K. Andersen, J. Phys. (Paris) **49**, C8-17 (1988).
[34] S. M. Valvidares, J. Dorantes-Dávila, H. Isern, S. Ferrer, and G. M. Pastor, Phys. Rev. B **81**, 024415 (2010).
[35] M. Zelený, M. Šob, and J. Hafner, Phys. Rev. B **79**, 134421 (2009).
[36] M. Tanveer, P. Ruíz-Díaz, and G. M. Pastor, Phys. Rev. B **87**, 075426 (2013).
[37] J. C. Tung and G. Y. Guo, Phys. Rev. B **83**, 144403 (2011).
[38] M. Saubanère, M. Tanveer, P. Ruíz-Díaz, and G. M. Pastor, Phys. Status Solidi B **247**, 2610 (2010).
[39] F. Schubert, Y. Mokrousov, P. Ferriani, and S. Heinze, Phys. Rev. B **83**, 165442 (2011).
[40] G. M. Pastor and J. Dorantes-Dávila, Phys. Rev. B **52**, 13799 (1995).
[41] G. Nicolas, J. Dorantes-Dávila, and G. M. Pastor, Phys. Rev. B **74**, 014415 (2006).
[42] Y. Kakehashi, Phys. Rev. B **31**, 3104 (1985).
[43] A. A. Aligia and T. Kroll, Phys. Rev. B **81**, 195113 (2010).
[44] A. A. Aligia, Phys. Rev. B **88**, 075128 (2013).